Contribution from the Department of Chemistry,
University of Minnesota, Minneapolis, Minnesota 55455

# 2D NMR Studies of Paramagnetic Diiron Complexes

Li-June Ming, Ho G. Jang, and Lawrence Que, Jr.*

*Received July 5, 1991*

Diiron complexes of dinucleating ligands have been demonstrated to be good structural and spectroscopic models for the diiron-oxo proteins. Although such complexes show relatively sharp isotropically shifted $^1$H NMR resonances due to their fast electronic relaxation rates, detailed assignment of their isotropically shifted $^1$H NMR resonances has thus far not been achieved due to the difficulty in establishing bond connectivities on paramagnetic complexes. In this report, we present 2D COSY, TOCSY, and EXSY studies of the complex $[Fe_2(BPMP)(O_2P(OPh)_2)_2]^{n+}$ (BPMP = 2,6-bis[(bis(2-pyridylmethyl)amino)methyl]-4-methylphenol; $n$ = 1, 2) in both its diferrous and mixed-valence states. The resonances due to the two distinct pyridine rings can be unambiguously assigned from the observation of bond-correlated cross signals in the 2D spectra due to the meta$_1$-para-meta$_2$ pyridyl proton connectivities. The 2D data used in connection with relaxation time measurements and the known crystal structure of the reduced complex allow the isotropically shifted proton resonances of the reduced complex to be conclusively assigned. The resonances of the diferrous and mixed-valence complexes can also be correlated by EXSY and saturation transfer experiments. This report represents the first detailed NMR study of model complexes for nonheme iron proteins by the use of 2D NMR techniques, demonstrating the versatility of NMR spectroscopy for the study of paramagnetic metal complexes.

Nuclear magnetic resonance (NMR) has been a valuable tool for the study of the ligand environments of many paramagnetic metal complexes through the detection and assignment of isotropically shifted proton resonances.[1] These NMR techniques have been applied for the study of several paramagnetic metalloproteins and have provided important information about the metal-binding sites in those proteins.[2] It has also been possible to monitor the interactions of substrates and inhibitors with some metalloenzymes and extract mechanistic information.[2] However, the application of 2D NMR techniques for the study of paramagnetic molecules has been impeded by the fast nuclear relaxation rates and the large range of isotropic shifts observed for such species. 2D NMR techniques such as COSY and TOCSY[3] would be particularly useful if bond-correlated cross signals (as a function of $\sin(\pi J_{ab}t_1)\exp(-t_1/T_2)$) due to the scalar coupling ($J_{ab}$) between pairs of nuclei could be observed; however, the line broadening observed for paramagnetic complexes renders the detection of such cross signals difficult in practice. Nevertheless, cross signals between pairs of scalarly coupled nuclei have recently been observed for synthetic complexes[4,5] and paramagnetic metalloproteins[6] with relatively sharp resonances.

Proton 2D exchange spectroscopy (EXSY) has become a valuable technique for the study of chemical exchange by showing exchange-correlated cross signals when all the individual resonances can be clearly observed (i.e. under relatively slow chemical exchange).[7] The application of EXSY for the study of paramagnetic species has also been difficult due to the fast nuclear relaxation rates that make the exchange-correlated cross signals almost impossible to observe when the longitudinal relaxation rate is much faster than the exchange rate, $T_1^{-1} \gg k_{ex}$. Nevertheless, EXSY has been successfully used for the study of relatively slow chemical exchange processes in simple paramagnetic complexes and of electron transfer in cytochrome $c_3$.[4,8]

In the past several years, a number of dinuclear iron complexes have been synthesized to mimic the active-site metal centers of nonheme iron proteins, such as hemerythrin, ribonucleotide reductase, purple acid phosphatases, and methane monooxygenase.[9,10] Previous NMR studies of the Fe(II)-Fe(II) and Fe(II)-Fe(III) complexes of the dinucleating ligand BPMP, e.g. $[Fe_2(BPMP)(OPr)_2]^{n+}$ (BPMP = 2,6-bis[(bis(2-pyridylmethyl)amino)methyl]-4-methylphenol; $n$ = 1, 2), showed many relatively sharp isotropically shifted resonances spread over a spectral width of 200-400 ppm.[11] Preliminary assignment of the resonances in these complexes was achieved on the basis of relaxation-time measurements.[11] It was, however, not possible to assign the various resonances to individual pyridine rings without the information regarding to the through-bond correlation of the pyridine resonances.

To demonstrate the suitability of using 2D NMR techniques for the study of these paramagnetic diiron complexes, we have chosen the reduced and mixed valence forms of the complexes $[Fe_2(BPMP)(O_2P(OPh)_2)_2]^{n+}$ ($n$ = 1, reduced; $n$ = 2, mixed valence) as a starting point. We present here 2D bond-correlation COSY and TOCSY studies for the identification of the two distinct pairs of pyridine rings in these 2-fold symmetric complexes. We also demonstrate the use of saturation transfer and 2D EXSY techniques to correlate the resonances of the reduced form with those of the mixed-valence form. These studies provide the means for detailed assignment of the isotropically shifted $^1$H resonances of these model complexes that should enhance our understanding of the solution structure of these models for dinuclear nonheme iron proteins.

## Experimental Section

All the chemicals were the highest grade from commercial sources and used as received. The solvents $CH_2Cl_2$ and $CH_3CN$ were distilled from $CaH_2$ under argon before use. The ligand BPMP was synthesized according to literature methods[12] and its mixed-valence Fe(II)Fe(III) complex with diphenyl phosphate bridges was prepared by procedures similar to the synthesis of analogous propionate complex.[11] Satisfactory elemental analyses (M. H. W. Laboratories, Phoenix, AZ) were obtained for $[Fe^{II}Fe^{III}(BPMP)(O_2P(OPh)_2)_2](ClO_4)_2\cdot CH_3OH$. Anal. Calcd for $C_{58}H_{57}Cl_2Fe_2N_6O_{18}P_2$: C, 50.82; H, 4.19; N, 6.13; P, 4.52. Found: C, 50.82; H, 4.26; N, 6.33; P, 4.47.

(1) La Mar, G. N.; Horrocks, W. DeW., Jr.; Holm, R. H.; Eds. *NMR of Paramagnetic Molecules, Principles and Applications*; Academic: New York, 1973.
(2) Bertini, I.; Luchinat, C. *NMR of Paramagnetic Molecules in Biological Systems*; Benjamin/Cummings: Menlo Park, CA, 1986.
(3) Ernst, R. R.; Bodenhausen, G.; Wokaun, A. *Principles of Nuclear Magnetic Resonances in One and Two Dimensions*; Oxford University: Oxford England, 1987.
(4) (a) Peters, W.; Fuchs, M.; Sicius, H.; Kuchen, W. *Angew. Chem., Int. Ed. Engl.* **1985**, *24*, 231-233. (b) Jenkins, B. G.; Lauffer, R. B. *Inorg. Chem.* **1988**, *27*, 4730-4738. (c) Jenkins, B. G.; Lauffer, R. B. *J. Magn. Reson.* **1988**, *80*, 328-336.
(5) (a) Luchinat, C.; Steuernagel, S.; Turano, P. *Inorg. Chem.* **1990**, *29*, 4351-4353. (b) Keating, K. A.; deRopp, J. S.; La Mar, G. N.; Balch, A. L.; Shiau, F. Y.; Smith, K. M. *Inorg. Chem.* **1991**, *30*, 3258-3263.
(6) (a) Yu, L. P.; La Mar, G. N.; Rajarathnam, K. *J. Am. Chem. Soc.* **1990**, *112*, 9527-9534. (b) de Ropp, J. S.; La Mar, G. N.; Wariishi, H.; Gold, M. H. *J. Biol. Chem.* **1991**, *266*, 15001-15008. (c) Banci, L.; Bertini, I.; Turano, P.; Tien, M.; Kirk, T. K. *Proc. Natl. Acad. Sci. U.S.A.* **1991**, *88*, 6956-6960.
(7) Perrin, C. L.; Dwyer, T. J. *Chem. Rev.* **1990**, *90*, 935-967.
(8) Santos, H.; Turner, D. L.; Xavier, A. V.; Le Gall, J. *J. Magn. Reson.* **1984**, *59*, 177-180.
(9) Que, L., Jr.; True, A. E. *Prog. Inorg. Chem.* **1990**, *38*, 97-200.
(10) (a) Kurtz, D. M., Jr. *Chem. Rev.* **1990**, *90*, 585-606. (b) Vincent, J. B.; Olivier-Lilley, G. L.; Averill, B. A. *Chem. Rev.* **1990**, *90*, 1447-1467.
(11) (a) Borovik, A. S.; Papaefthymiou, V.; Taylor, L. F.; Anderson, O. P.; Que, L., Jr. *J. Am. Chem. Soc.* **1989**, *111*, 6183-6195. (b) Borovik, A. S.; Hendrich, M. P.; Holman, T. R.; Münck, E.; Papaefthymious, V.; Que, L., Jr. *J. Am. Chem. Soc.* **1990**, *112*, 6031-6038.
(12) Suzuki, M.; Kanatomi, H.; Murase, I. *Chem. Lett., Chem. Soc. Jpn.* **1981**, 1745-1748.

0020-1669/92/1331-0359$03.00/0 

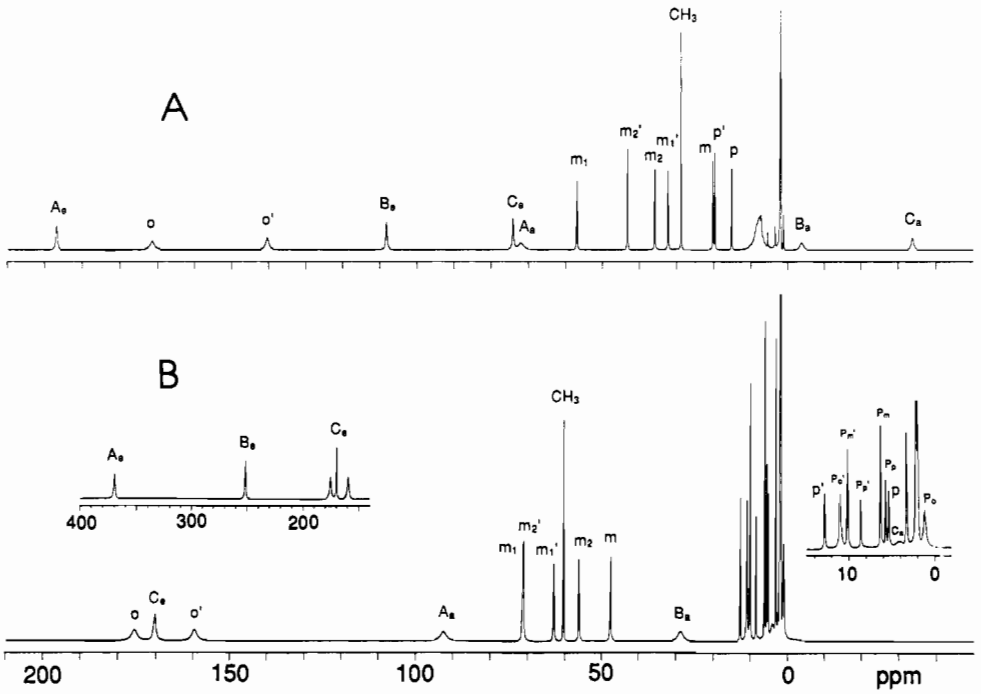


**Figure 1.** Proton NMR spectra (300 MHz and 35 °C) of (A) the reduced and (B) the mixed-valence $[Fe_2(BPMP)(O_2P(OPh)_2)_2]^{n+}$ complex in $CD_3CN$. The assignment of the resonances is carried out using 2D techniques and by correlation of the relaxation times with the crystal structure of the reduced complex. The broad signal at ~8 ppm in part A is due to the ring protons on the bridging diphenyl phosphate resulting from fast interchange of the phenyl rings (see text).

The reduced $Fe^{II}Fe^{II}$ complex was prepared as follows. To 0.200 g (0.377 mmol) of HBPMP in 15 mL of methanol was added 0.254 g (0.754 mmol) of $Fe(BF_4)_2 \cdot 6H_2O$ in 10 mL methanol under anaerobic conditions to form a dark yellow solution. A 0.236-g (0.943-mmol) sample of phosphoric acid, diphenyl ester, and 0.13 mL (0.943 mmol) of triethylamine were added to the above solution to yield a yellow precipitate, which was filtered and recrystallized from acetone/$CH_2Cl_2$, yielding $[Fe^{II}Fe^{II}(BPMP)(O_2P(OPh)_2)_2](BF_4)$. Anal. Calcd for $C_{57}H_{53}BF_4Fe_2N_6O_9P_2$: C, 55.82; H, 4.36; N, 6.85; P, 5.05. Found: C, 55.70; H, 4.37; N, 6.90; P, 5.29. This complex was also characterized by cyclic voltammetry in acetonitrile exhibiting potentials of +150 and +760 mV vs SCE, similar to the earlier reported values of +135 and +755 mV.[13] Characterization of the reduced complex by $^{57}Fe$ Mössbauer and EPR spectroscopies, magnetic susceptibility, and X-ray crystallography will be presented elsewhere.[14]

Varian VXR300 and IBM NR/300 spectrometers were used for collection of both 1D and 2D $^1H$ NMR spectra. The 1D spectra were obtained using a 90° pulse (10–12 μs) with 16K data points. An inversion–recovery pulse sequence (180°–$\tau$–90°–AQ) was used to obtain nonselective proton longitudinal relaxation times ($T_1$) with the carrier frequency set at several different positions to ensure the validity of the measurements.

A typical magnitude COSY spectrum was collected with 1024 data points in $t_2$ and 512 data points in $t_1$ with a bandwidth of 18–27 kHz and a repetition time of <0.1 s. The time for the data collection for a 10-mM sample was about 30 min. A zero-degree shifted sine bell combined with a Gaussian function to give a maximum at one-fourth the acquisition time was applied in both dimensions and zero-filled to 2048 $t_2$ × 2048 $t_1$ data points prior to Fourier transformation and symmetrization. In this study, cross signals from pairs of signals with $\Delta\delta < 1$ ppm in a spectral width of ~95 ppm could be clearly recognized under proper processing procedures.

TOCSY experiments were performed using the same parameters used for the COSY experiments under the same experimental conditions, except that the second 90° pulse in the COSY sequence was replaced by an MLEV-17 pulse sequence for spin locking.[15] A mixing time of ~10 ms was found to give 2D spectra with easily observed bond-correlated cross signals. Data processing for the TOCSY experiments to give magnitude-mode spectra was also similar to that in the COSY experiments.

EXSY experiments were performed using the conventional NOESY 90°–$t_1$–90°–$t_{mix}$–90°–AQ phase-sensitive pulse sequence with 1024 $t_2$ and 512 $t_1$ data points. Both dimensions were apodized by a combined sine bell–Gaussian window function, zero-filled to 2048 $t_2$ × 2048 $t_1$ data points, and Fourier transformed to give peaks in absolute-value mode. The validity of the EXSY results in this study was further confirmed by 1D saturation-transfer techniques.

The 1D saturation-transfer experiments were performed by selective presaturation of a signal of interest using the decoupler for a short period of time (<0.1 s) followed by a direct subtraction of the FID with the decoupler set at a reference position. Blocks of 40 transients were accumulated for each until a sufficient signal-to-noise ratio for the difference spectrum was achieved. Saturation transfer between resonances with relaxation times as short as ~1 ms can be clearly detected by this method, but it is practically impossible to observe it by the EXSY method.

## Results and Discussion

The $^1H$ NMR spectrum of the reduced $[Fe_2BPMP(O_2P(OPh)_2)_2]^+$ complex shows well resolved isotropically shifted resonances spread out over 240 ppm (Figure 1A). The meta and para protons on the pyridine rings and the bridging phenolate ring show relatively sharp features in the ~20–60 ppm region and can be easily assigned on the basis of their chemical shifts and relaxation times. The resonances at >20 ppm have $T_1$ values of ~15 ms and can be assigned to the phenolate and pyridyl meta ring protons, while the two resonances at ~20 ppm with $T_1$ of >30 ms are assigned to the para pyridyl protons. However, these resonances cannot be specifically assigned to individual pyridyl rings at this stage based on the above criteria. The observation of eight isotropically shifted resonances for the four pyridine rings (as well as only one meta signal for the bridging phenolate) suggests that the complex has 2-fold symmetry in acetonitrile solution. The bridging diphenyl phosphate proton resonances, however, are not resolved and appear as a broad signal centered at ~8 ppm, suggesting that there is an equilibrium among different conformations occurring at an intermediate exchange rate.

A total of six methylene resonances are observed for the 12 methylene protons in $[Fe_2BPMP(O_2P(OPh)_2)_2]^+$ (labeled $A_a$, $A_e$, $B_a$, $B_e$, $C_a$, and $C_e$ in Figure 1A), which indicates that all the protons in the half-molecule have different magnetic environments. The difference in isotropic shifts for the geminal methylene pairs arises from their involvement in chelate ring formation, affording different Fe–N–C–H dihedral angles and consequently different

(13) Schepers, K.; Bremer, B.; Krebs, B.; Hennkel, G.; Althaus, E.; Mosel, B.; Müller-Warmuth, W. *Angew. Chem., Int. Ed. Engl.* **1990**, *29*, 531–533.
(14) Jang, H. G.; Que, L. Jr. Manuscript in preparation.
(15) Bax, A.; Davis, D. G. *J. Magn. Reson.* **1985**, *65*, 355–360.

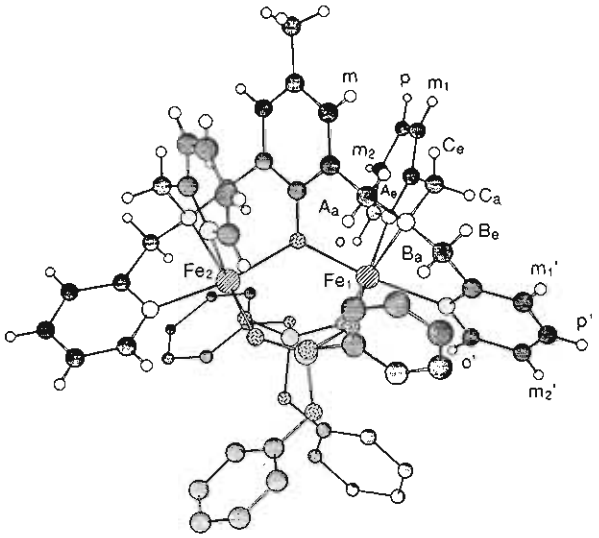


**Figure 2.** Plot of the diferrous complex $[Fe_2(BPMP)(O_2P(OPh)_2)_2]^+$ obtained by X-ray crystallography.[14] This complex has a pseudo-2-fold symmetry with one of the pyridine rings in the half-molecule trans to the $\mu$-phenoxo and the other pyridine ring trans to one of the diphenyl phosphate bridges (in the front of the complex). The other diphenyl phosphate bridge (at the back of the complex) is trans to the tertiary amine nitrogen. The methylene protons with a subscript e are in the equatorial positions (i.e. with the Fe–N–C–H dihedral angle near 180°) while those with a subscript a are in the axial positions.

amounts of spin delocalization. In early studies of diamine complexes of paramagnetic transition-metal ions, the geminal methylene protons were found to shift differently with the equatorial-like proton (i.e. with the M–N–C–H dihedral angle close to 180°) shifted further downfield.[16] The equatorial protons have longer Fe–H distances and thus show sharper resonances and longer relaxation times. Indeed, three of the six methylene proton resonances in the diferrous complex at 196.8, 108.1, and 74.0 ppm are sharper ($\Delta\nu_{1/2} < 150$ Hz) with $T_1$ values of ~3 ms as compared to the other three at 72.0, −3.9, and −33.8 ppm which have $\Delta\nu_{1/2} > 200$ Hz and $T_1$ values of ~1 ms (Figure 1A). The sharper resonances ($A_e$, $B_e$, and $C_e$) are assigned to the methylene protons in equatorial-like positions and the broad resonances ($A_a$, $B_a$, and $C_a$) are due to the protons at the axial-like positions. The larger isotropic shift of signal $A_e$ compared to those of $B_e$ and $C_e$ suggests that the proton $A_e$ has an Fe–N–C–H dihedral angle closer to 180° than the other equatorial-like protons $B_e$ and $C_e$.

The crystal structure of the reduced complex[14] shows that the methylene group attached to the phenolate ring (Ph–$CH_2$) has two distinct Fe–N–C–H dihedral angles (176.7 and 57°) with the equatorial proton ($A_e$) nearly in the Fe–N–C plane (Figure 2). The other two methylene groups attached to the pyridine rings (py–$CH_2$) also have similar conformations (166, −74.3°; 148, −93°) with the protons $B_e$ and $C_e$ in the equatorial-like positions (Figure 2). The farthest downfield shifted resonance $A_e$ of 196.8 ppm is thus assigned to the equatorial Ph–$CH_2$ proton since it is nearly in the Fe–N–C plane. There are broad resonances at 171.5 and 140.3 ppm which are further downfield shifted than the two equatorial methylene resonances $B_e$ and $C_e$; these two resonances cannot be due to the axial methylene protons, which would exhibit relatively small downfield shifts, and are thus assigned to the ortho protons on the two distinct pyridine rings. The assignment of the Ph–$CH_2$ proton resonances has been further confirmed by deuteration.

The mixed-valence $[Fe_2BPMP(O_2P(OPh)_2)_2]^{2+}$ complex shows a $^1H$ NMR spectrum that has twice the isotropic shift range observed for the diferrous complex (Figure 1B). The larger isotropic shifts of this complex are presumably due to the presence of the more paramagnetic high-spin Fe(III) center. Like that of the diferrous form, the $^1H$ NMR spectrum of this complex shows one resonance for the bridging phenolate meta protons and eight peaks for the pyridyl ring protons, indicating that there is effective 2-fold symmetry for the complex in acetonitrile solution. Thus the rate of intramolecular electron transfer in the mixed-valence diiron center is faster than the NMR time scale and is estimated to be $>10^5$ $s^{-1}$ based on a $\Delta\delta$ of 400 ppm calculated for the $A_e$ proton bound respectively to an Fe(II) center and an Fe(III) center. The methylene protons in the mixed-valence complex have features similar to those in the reduced complex: (a) the 12 methylene protons are resolved into six signals indicative of a 2-fold symmetry; (b) three relatively sharper methylene resonances due to the protons in the equatorial positions are more downfield shifted than the broad "axial" protons. In contrast to the diferrous form, the bridging diphenyl phosphate features of the mixed-valence form are well resolved in the region ~0–12 ppm, suggesting a greater conformational rigidity for the four phenyl rings in the latter complex. Only six resonances are observed, three each for the inner and outer phenyl rings.

Further assignment for these spectra cannot be made without selective deuteration or establishing bond connectivities. The latter can in principle be established using COSY techniques. It is difficult to observe coherent magnetization transfer among nuclei with broad resonances (such as in paramagnetic systems that give extremely small $\exp(-t_1/T_2)$ values); however, as the resonances become sharper, the possibility for the observation of coherent magnetization transfer improves and cross signals may indeed be observed in a 2D NMR spectrum.[4,6] We have successfully applied the conventional COSY technique to the reduced form of the $Fe_2$BPMP complex and found cross signals in the 2D spectrum due to through-bond connectivities among protons within a spectral width of ≥50 ppm (Figure 3A). For example, the signal $m_1$ ($m_1'$) shows a cross signal to the signal $p$ ($p'$), which in turn shows a cross signal to the signal $m_2$ ($m_2'$). These connectivities establish the signals $m_1$, $p$, and $m_2$ as the meta and para protons of one type of pyridine, while the signals $m_1'$, $p'$, and $m_2'$ arise from the other type of pyridine.

Although methylene protons always show large geminal coupling, we did not observe any coherent magnetization transfer between the geminal protons in the COSY spectrum of the diferrous complex with a spectral width of >200 ppm, while the pyridine connectivities were still clearly observed. The broadness of the methylene signals makes such cross signals rather difficult to observe.

Signal assignments can also be achieved using TOCSY (Figure 3B), which shows four cross signals for the meta and para protons of each pyridine ring. In contrast to the COSY technique where the 180° out-of-phase cross-peak multiplets partially cancel and cause a reduction in signal intensities, TOCSY affords cross-peak multiplets in the nearly in-phase absorption mode and thus may be more feasible for detecting bond-correlated coherent magnetization transfer among broad resonances.[15] We have noticed that the TOCSY experiment indeed reveals cross signals with higher intensities as compared to those in the COSY experiment under the same experimental conditions and using the same techniques of data manipulation. Parts C–F of Figure 3 are the traces obtained from the 2D experiments, which clearly show that the cross signals in the TOCSY spectrum have much higher signal-to-noise ratios. However, due to the inefficiency of the spin-lock field in covering the wide spectral region (>15 000 Hz), coherent magnetization transfer between signals farther away from the carrier frequency does not occur to its full extent, thus resulting in cross signals with smaller intensities (Figure 3F; the signal at ~60 ppm).

The mixed-valence complex exhibits relatively sharp ring proton resonances in the region ~0–70 ppm with the para pyridyl proton resonances overlapped with the six resonances due to the phenyl protons of the bridging phosphates in the 0–15 ppm region (Figure 1B). Despite the large spectral width involved, the 2D COSY spectrum of the complex reveals the para protons at 12.5 and 5.0 ppm to be correlated with the meta proton signals in the region >55 ppm, thus differentiating the resonances due to the two different types of pyridines (Figure 4A). The assignment of the

(16) Holm, R. H.; Hawkins, C. J. In ref 1, Chapter 7.

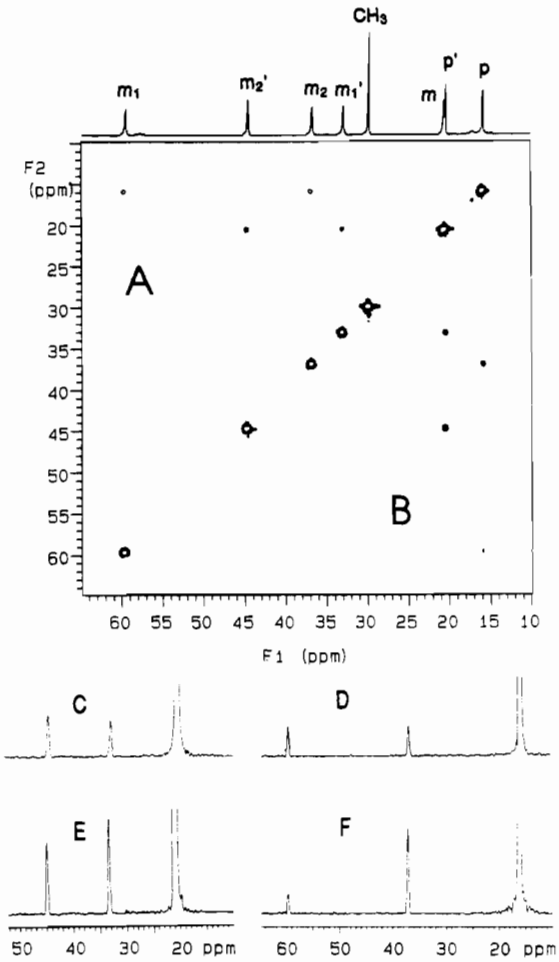


**Figure 3.** Proton homonuclear COSY (A) and TOCSY (B) spectra of the reduced complex $[Fe_2(BPMP)(O_2P(OPh)_2)_2]^+$ in $CD_3CN$ at 300 MHz and 25 °C. The two spectra were obtained using 1024 $t_2$ and 512 $t_1$ data points and apodized by the use of an identical combined sine bell–Gaussian function and zero-filled to 2K $t_2 \times$ 2K $t_1$ data points prior to Fourier transformation and symmetrization. Parts C–F are the traces of the para protons in the COSY (C and D) and the TOCSY (E and F) spectra with the para proton signals set to the same height. The cross signals in the TOCSY experiment show larger intensities relative to those in the COSY experiment. The smaller cross signal at ~60 ppm in F may be due to the inefficiency of the spin-lock field.

resonances at ~0–12 ppm due to the bridging diphenyl phosphates can also be achieved using COSY and TOCSY (Figure 4) where four cross signals are detected due to the ortho–meta–para connectivities. The signals at 10.7 and 0.9 ($P_{o'}$ and $P_o$), 9.9 and 6.0 ($P_{m'}$ and $P_m$), and 8.3 and 5.4 ppm ($P_{p'}$ and $P_p$) can be therefore assigned to the phenyl ortho, meta, and para protons of the bridging diphenyl phosphate, respectively. It is interesting to note that one set of peaks is shifted downfield, while the other set is shifted upfield; we attribute this difference to dipolar effects of the Fe(II) center. The resonances $P_o$, $P_m$, and $P_p$ with relaxation times of 3.9, 31, and 63 ms, respectively, are assigned to the outside phenyl rings (the upper two rings in Figure 2) which have slightly shorter Fe–H distances than those of the two inside rings (the two rings in the bottom of Figure 2 that give signals $P_{o'}$, $P_{m'}$, and $P_{p'}$ with $T_1$ of 6.5, 35, and 64 ms, respectively).

In paramagnetic metal complexes, the metal–proton distances ($r_{M-H}$) can be correlated to the proton relaxation rates according to the Solomon equation (eq 1),[17] where $C$ is a collection of

$$T_{1M}^{-1} = C[S(S+1)]r_{M-H}^{-6}f(\tau_c,\omega) \quad (1)$$

physical constants and $f(\tau_c,\omega)$ is the correlation function. In a system of two paramagnetic centers wih negligible magnetic interaction between the two paramagnetic centers, the paramagnetic relaxation of a proton derives from both metal centers (eq 2).[2]

$$T_{1Mobs}^{-1} = T_{1Ma}^{-1} + T_{1Mb}^{-1} \quad (2)$$

$$T_{1Mobs}^{-1} = C[S(S+1)](r_{M-H}^{-6} + r_{M'-H}^{-6})f(\tau_c,\omega) \quad (3)$$

$$T_{1Mcalc}^{-1} = T_{1Mref}^{-1}[(r_{M-H}^{-6} + r_{M'-H}^{-6})/(r_{M-H}^{-6} + r_{M'-H}^{-6})_{ref}] \quad (4)$$

This equation can be further simplified to eq 3 when the two paramagnetic centers are identical. Accordingly, the relaxation rates ($T_{1Mobs}^{-1}$) can be calculated on the basis of crystal structure information (giving the $r_{M-H}^{-6}$ values) with respect to that of a reference resonance ($T_{1Mref}^{-1}$) as shown in eq 4.

The magnetic interactions between the two Fe(II) ions in analogous diferrous complexes and proteins have been found to be small.[9] This weak magnetic interaction, while not limiting the use of eqs 2–4 for correlation of relaxation data with structure in the diferrous complex, may decrease the Fe(II) electronic relaxation times[2] and engender the observation of sharper isotropically shifted resonances with larger $T_1$ values (Figure 1 and Table I) relative to mononuclear Fe(II) complexes. We have applied eqs 2–4 to correlate the NMR relaxation data with the Fe–H distances in the reduced complex. The two types of pyridine rings revealed by the 2D experiments are also distinguished by the X-ray crystallographic study.[14] However, when eq 1 alone is used to correlate the relaxation rates with the Fe–H distances using one of the para protons as the reference, the two types of pyridines cannot be differentiated from each other as similar $T_1$ values are calculated ($T_{1calc}'$, Table I). This poor correlation can be greatly improved when eqs 2–4 are applied by the introduction of the contribution of the second Fe(II) to the relaxation ($T_{1calc}$, Table I). Indeed, a smaller $\sum(T_{1calc} - T_{1expt})^2$ value is obtained when the second Fe(II) is taken into account in the calculations. The calculated $T_1$ values for the two types of pyridine rings become distinct with the ones trans to the $\mu$-phenoxo bridge (which give slightly longer $r_{M-H}$ distances) possessing longer $T_1$ values consistent with the experimental $T_1$ values (Figure 2 and Table I). The calculated $T_1$ values for the methylene protons are also consistent with the experimental values showing distinct $T_1$'s for the axial and equatorial geminal protons. The assignment of the

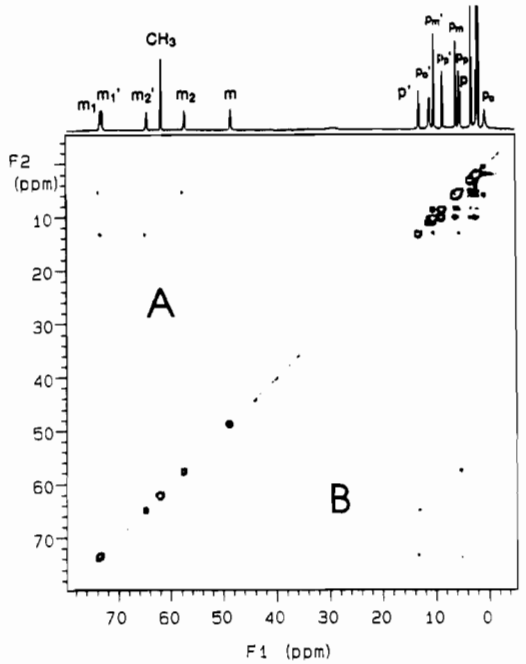


**Figure 4.** Proton homonuclear COSY (A) and TOCSY (B) spectra of the mixed-valence complex $[Fe_2(BPMP)(O_2P(OPh)_2)_2]^{2+}$ in $CD_3CN$ at 300 MHz and 25 °C. The spectra were obtained in a manner similar to those in Figure 3. The smaller intensity of the cross signals in this complex as compared to that in the diferrous complex (Figure 3) is due to the smaller nuclear relaxation times in the former complex (Table I).

(17) Solomon, I. *Phys. Rev.* **1955**, *99*, 559–565.

**Table I.** NMR Parameters and the Experimental and Calculated Relaxation Times of the Reduced $[Fe_2(BPMP)(O_2P(OPh_2)_2)]^+$ Complex[a,b]

| signal | shift, ppm | $\Delta\nu_{1/2}$,[c] Hz | $Fe_1$–H, Å | $Fe_2$–H, Å | $T_{1calc}$',[d] ms | $T_{1calc}$,[e] ms | $T_{1expt}$,[c] ms |
|---|---|---|---|---|---|---|---|
| | | | Pyridine trans to $O_2P(OPh_2)_2$ | | | | |
| $m_1$ | 56.8 (71.0) | 40 (*f*) | 5.016 | 7.295 | 12.7 | 13.5 | 13 (9.2) |
| $p$ | 15.1 (5.0) | 20 (27) | 5.852 | 7.770 | 32[g] | 32[g] | 32 (22) |
| $m_2$ | 35.8 (55.8) | 31 (60) | 5.189 | 6.839 | 15.5 | 15.4 | 14 (9.2) |
| $o$ | 171.5 (175.4) | 418 (490) | 3.219 | 5.091 | 0.88 | 0.98 | 0.9 (1.0) |
| | | | Pyridine Trans to $\mu$-Phenoxo | | | | |
| $m_1'$ | 32.3 (62.7) | 33 (60) | 5.026 | 8.275 | 12.8 | 14.4 | 15 (8.7) |
| $p'$ | 19.6 (12.6) | 18 (27) | 5.886 | 9.337 | 33.1 | 36.8 | 49 (21.2) |
| $m_2'$ | 43.2 (70.8) | 28 (*f*) | 5.221 | 8.582 | 16.0 | 18.1 | 22 (10.5) |
| $o'$ | 140.3 (150.3) | 296 (488) | 3.228 | 6.420 | 0.95 | 1.04 | 1.1 (1.0) |
| | | | Phenolate–$CH_2$[h] | | | | |
| $A_e$ | 196.8 (370) | 151 (380) | 3.930 | 5.408 | 2.90 | 3.01 | 2.7 (1.9) |
| $A_a$ | 72.0 (92.2) | 515 (543) | 3.118 | 4.075 | 0.73 | 0.72 | 0.9 (0.7) |
| | | | $CH_2$ of Pyridine Trans to $\mu$-Phenoxo[h] | | | | |
| $B_e$ | 108.1 (251.2) | 127 (290) | 3.832 | 6.616 | 2.51 | 2.86 | 3.0 (1.9) |
| $B_a$ | −3.9 (28.4) | 361 (482) | 3.155 | 5.538 | 0.78 | 0.89 | 1.0 (0.84) |
| | | | $CH_2$ of Pyridine Trans to $^-O_2P(OPh)_2$[h] | | | | |
| $C_e$ | 74.0 (170.1) | 111 (216) | 3.831 | 6.344 | 2.51 | 2.82 | 3.1 (2.5) |
| $C_a$ | −33.8 (3.8) | 220 (*f*) | 3.420 | 6.654 | 1.27 | 1.47 | 1.6 (0.84) |

[a] Obtained at 300 MHz and 35 °C in $CD_3CN$ (Figure 1). The numbers in parentheses are the values for the correlated signals in the mixed-valence complex. [b] The assignment is based on the 2D experiments and relaxation times. [c] The line widths of all the resonances are smaller at 25 °C suggesting that the complexes become less rigid at higher temperature. [d] The $T_1$ value is obtained by considering only one Fe(II) ($Fe_1$–H distances). [e] The $T_1$ value is obtained by taking into account both $Fe_1$–H and $Fe_2$–H distances using eqs 2–4. [f] Signal not resolved. [g] This resonance is taken as the reference for $T_1$ calculations. [h] $CH_e$, the methylene proton at the "equatorial" position; $CH_a$, the methylene proton at the "axial" position.

−33.8 ppm resonance to the axial proton of the pyridyl methylene trans to the phosphate bridge, which has the longest Fe–H distance of the three axial protons, is also consistent with the relatively larger $T_1$ value (1.6 ms vs ~1 ms) for this resonance.

A 1:1 mixture of the reduced and the mixed-valence forms of the $[Fe_2BPMP(O_2P(OPh)_2)_2]^{n+}$ complex shows isotropically shifted proton resonances attributable to both oxidation states. The observation of the well-resolved resonances suggests that the electron transfer between the two oxidation states, if it occurs, is slow with respect to the NMR time scale. Chemical exchange-induced saturation transfer can easily be monitored by 2D techniques when the longitudinal nuclear relaxation rates of the exchanging nuclei are slower than the exchange rate.[4,7] The NOESY pulse sequence (90°–$t_1$–90°-$t_{mix}$–90°–ACQ) is commonly used for the observation of chemical exchange (therefore designated as EXSY), since it cannot differentiate dipole–dipole interactions (which cause the nuclear Overhauser effect) from the chemical exchange-induced magnetization transfer.[7] By using a mixing time of 10 ms ($<T_1$'s of the ring protons) in the EXSY experiments, all the exchange partners for the ring protons are revealed by exchange cross signals (Figure 5A). Thus the correlation of the proton resonances in the reduced complex with those in the mixed-valence complex is obtained. The observation of exchange cross signals in the 1:1 mixture also suggests that electron transfer does occur between the two oxidation states, albeit at a slow rate.

The electron-transfer rate between the two oxidation states can be estimated by the use of saturation-transfer techniques. When a resonance of the mixed-valence complex in the 1:1 mixture is saturated, the decay of the signal intensity of the corresponding diferrous signal ($M_z^R$) as a function of the irradiation duration time $t$ with respect to its intensity at equilibrium state ($M_0^R$) is given by eq 5.[18] When the signal of the mixed-valence form is

$$M_z^R = M_0^R[(\tau_{1R}/\tau_R)\exp(-t/\tau_{1R}) + (\tau_{1R}/T_{1R})] \quad (5)$$

saturated with a long irradiation time (~0.1 s), the intensity of the corresponding signal in the diferrous form can be represented as in eq 6, and the value $\tau_{1R}$ ($\tau_{1R}^{-1} = T_{1R}^{-1} + \tau_R^{-1}$ with the $\tau_R$

$$M_z^R(t \to \infty) = M_0^R(\tau_{1R}/T_{1R}) \quad (6)$$

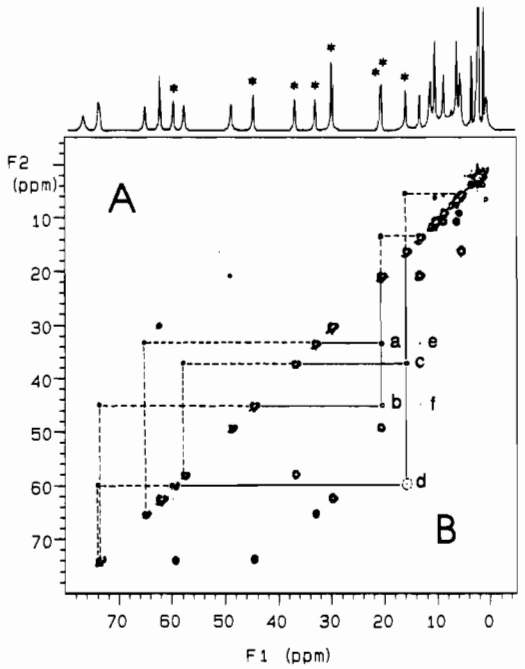


**Figure 5.** Proton EXSY (A) and TOCSY (B) spectra of a 1:1 mixture of the reduced and mixed-valence $[Fe_2(BPMP)(O_2P(OPh)_2)_2]^{n+}$ complexes (4 mM each in $CD_3CN$). The signals marked by asterisks in the 1D spectrum are due to the reduced complex. Cross signals observed in both spectra correlate the exchange proton pairs between the two complexes because of electron transfer. The TOCSY spectrum also shows bond-correlated cross signals (a–d) for the reduced complex as observed in Figure 3. Bond-correlated cross signals of the mixed-valence complex are not shown due to their poor signal-to-noise ratio. However, a bond correlation of the resonances of the mixed-valence complex can be obtained in the 1:1 mixture via the bond-correlated cross signals of the reduced complex (solid lines) and the exchange cross signals (dashed lines). The signals e and f are secondary bond-correlated TOCSY cross signals caused by the chemical exchange. These spectra also reveal that the two phenyl rings on the bridging phosphate ligands exchange with each other by showing cross signals for the ring protons.

as the lifetime of the reduced form) can be obtained. Alternatively, measurement of the change in signal intensity in the mixed-valence form upon saturation of a signal in the diferrous form can also provide the same information. Thus the intermolecular electron

(18) (a) Forsén, S.; Hoffman, R. A. *Acta Chem. Scand.* **1963**, *17*, 1787–1788. (b) Forsén, S.; Hoffman, R. A. *J. Chem. Phys.* **1963**, *39*, 2892–2901.

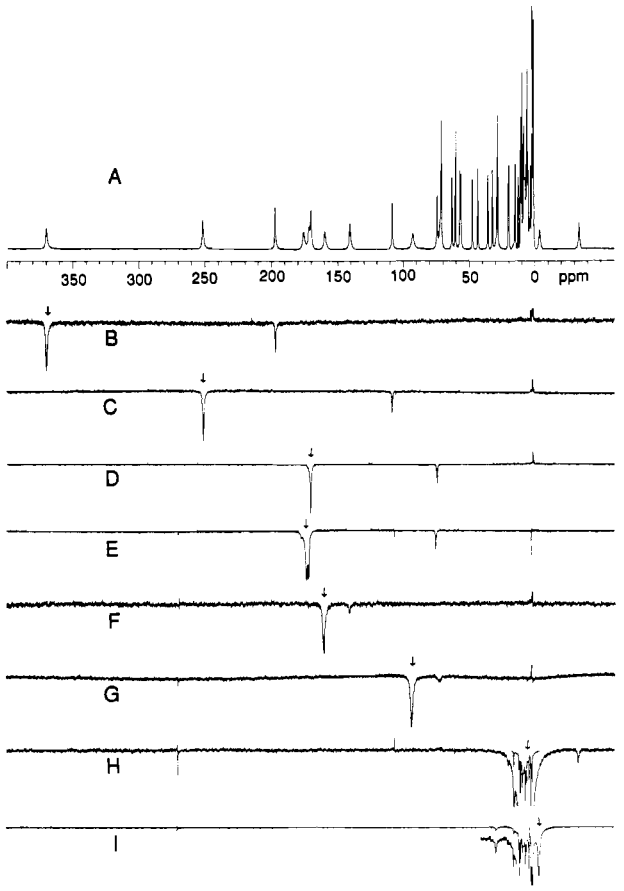


**Figure 6.** 1D saturation transfer experiments (300 MHz, 35 °C) on a 1:1 mixture of the reduced and mixed-valence $[Fe_2(BPMP)(O_2P(OPh)_2)_2]^{n+}$ complexes. By the use of a 10–30 ms presaturation pulse (marked by an arrow) on the signals $A_e$ (B), $B_e$ (C), $C_e$ (D), *o* (E), *o'* (F) $A_a$ (G), $B_a$ (H) and $C_a$ (I) of the mixed-valence complex (except E and I in which irradiation is on the signal of the reduced complex), their exchange partners can be unambiguously identified. In part E, the signal at 171.5 ppm of the reduced form is saturated with the reference set at a symmetric position downfield with respect to the signal at 175.4 ppm of the mixed valence form. Saturation transfer between the two signals is shown by the detection of the 175.4-ppm signal as a shoulder. The signal at 74 ppm in part E is due to saturation transfer from the partially saturated signal at 170.1 ppm as in part D.

transfer rate can be estimated by measuring $\tau_{1R}$ and $T_{1R}$. Calculations based on the experiments on the meta and para ring protons and the "equatorial" methylene protons give a $\tau_R$ value of 9.8 ± 1.8 ms, corresponding to an intermolecular electron-transfer rate of $(2.6 \pm 0.5) \times 10^4$ $M^{-1}$ $s^{-1}$.

The EXSY spectrum reveals that the two phenyl rings on the bridging phosphates also exchange with each other by showing cross signals between the two rings for the meta and the para protons. The ortho proton partners, however, do not show cross signals when a mixing time of 10 ms is used due to their short nuclear relaxation times (6.5 and 3.9 ms). This observation suggests that exchange of the bridging diphenyl phosphates also occurs in the mixed-valence complex, although to a lesser extent relative to the case in the reduced complex in which all the phenyl protons collapse into a broad resonace. By the use of the saturation transfer technique and eq 6, the rate of the interchange $(1/\tau_R)$ between the two phenyl rings is estimated to be 0.7 $s^{-1}$ for the mixed-valence complex alone. This intramolecular interchange rate for the mixed-valence complex increases 60-fold (40 $s^{-1}$) in the 1:1 mixture and is facilitated by the intermolecular electron-transfer equilibrium with the reduced complex, which has a significantly faster phenyl interchange rate. The addition of diphenyl phosphate to the mixed-valence complex results in the observation of only a small saturation transfer to the free ligand. This result suggests that ligand exchange is only a minor pathway for ring exchange; the major pathway must then be an intramolecular exchange process.

The presence of chemical exchange in a molecule may complicate its TOCSY spectrum by showing extra cross signals that are due to the exchange. Figure 5B is a TOCSY spectrum of the 1:1 mixture, in which the exchange signals can be recognized by comparison with Figure 5A. In addition, six more cross signals (signals a–f) are detected. Signals a–d are due to the through-bond connectivities of the pyridine ring protons in the reduced complex as observed in Figure 3, while the signals e and f are secondary bond-correlated cross signals between the corresponding ring protons of the reduced and the mixed-valence complexes due to the chemical exchange. Cross signals are also detected for the bridging diphenyl phosphate of the mixed-valence complex similar to those observed in its COSY and TOCSY spectra (Figure 4). The bond-correlated cross signals due to the ring protons of the mixed-valence complex are not observed in this plot because of their smaller intensities as shown in the TOCSY experiments of the mixed-valence complexes (Figure 4B). The capability of TOCSY to detect both coherent and chemical-exchange magnetization transfer in the 1:1 mixture allows us not only to assign the pyridyl ring protons via the bond-correlated cross signals (which are observed for the diferrous form, solid lines in Figure 5) but also to correlate the signals in the two oxidation states via the TOCSY-detected exchange cross signals (dashed lines in Figure 5).

The fast longitudinal relaxation rates of the methylene and the pyridyl ortho protons do not allow the EXSY technique to correlate the proton resonances from both oxidation states; however, such correlations can be accomplished with 1D saturation-transfer techniques. By the use of a presaturation pulse of 10–30 ms, exchange correlations can be observed to a large extent (>20%) for the "equatorial" methylene resonances with relatively long relaxation times (Figure 6B–D). The exchange correlation for the ortho pyridine protons and the "axial" methylene protons can also be observed, although to a smaller extent (<10%) due to their much faster relaxation rates (Figure 6E–I). Along with the EXSY and TOCSY results (Figure 5), a full correlation of the isotropically shifted resonances of the two oxidation states can be made (Table I).

Although paramagnetic Fe(II/III) complexes in many cases afford observable NMR signals, detailed assignment of their NMR spectra is not easily achieved, most studies relying on the application of the Solomon equation (eq 1). 2D NMR techniques have been almost exclusively used for structure studies of diamagnetic molecules; however, such techniques should be applicable for paramagnetic metal complexes with relatively sharp isotropically shifted resonances, despite the collapse of the spin multiplets and the quenching of the NOE due to the paramagnetism of such complexes. We have shown in this report that 2D NMR techniques can indeed be useful tools for signal assignment in paramagnetic diiron complexes. A better understanding of the structure–spectral correlation in these model systems should enhance the prospects of applying such spectroscopic methods for the further study of corresponding enzyme systems.

**Acknowledgment.** This work has been supported by the National Institutes of Health, Grant GM-38767. The Varian NMR spectrometer was purchased from funds provided by the National Institutes of Health, the National Science Foundation, and the University of Minnesota. We thank Dr. Theodore R. Holman for providing the deuterated BPMP ligand.

**Registry No.** $[Fe_2(BPMP)(O_2P(OPh)_2)_2]^+$, 126876-03-7; $[Fe_2(BPMP)(O_2P(OPh)_2)_2]^{2+}$, 126875-99-8.